Electronic Supplementary Information

Microwave-assisted synthesis of dual responsive ped nanohydroxyapatite for biomedical applications

Mohammad Irfan,[a] Ashok Jeshurun,[b] Bogala Mallikharjuna Reddy*[c 1]

[a]Department of Chemical Engineering, Indian Institute of Technology Tirupati, AP, 517619, India.

[b]Department of Mechanical Engineering, Indian Institute of Technology Madras, TN, 600036, India.

[c]Center for Research, Innovation, Development, and Applications, Jaiotec Labs (OPC) Private Limited, Amaravati, AP, 522503, India.

*Corresponding author Email: mrbogala@crimson.ua.edu
Tel: +91-9000097382

S 1. Fourier transform infrared spectroscopy

The FT-IR spectra of HAp, Nd:HAp, Dy:HAp, and Nd:Dy:HAp samples were acquired, from 400 cm^{-1} to 4000 cm^{-1}, to identify the important functional groups (PO_4^{3-} and OH^-) present in the chemical structures. The FT-IR spectra of all the HAp samples are displayed in Fig. S1. The spectra displayed the characteristic peaks at 985-1098 cm^{-1}, 965-970 cm^{-1}, and 570-610 cm^{-1}. They represent the fingerprint regions for vibrational modes of O–P–O bonds, i.e., antisymmetric stretching (v_3), symmetric stretching (v_1), and bending (v_4), that corresponds to the PO_4^{3-} of HAp, respectively.[1,2] It was found that the doubly degenerated v_2 bending vibration was linked to the peak at 477 cm^{-1}. The signal detected at 967 cm^{-1} was attributed to the phosphate group's symmetric stretching mode of v_1.[1,2] The peaks located at ~1000 cm^{-1} resulted from an asymmetric v_3 stretching vibration that was triply degenerated. For the O–P–O bond, the peaks measured at ~ 586 cm^{-1} were found to represent a v_4 bending mode. The distinctive peak of the hydrogen phosphate group was located in the band at 878 cm^{-1} .[1,2]

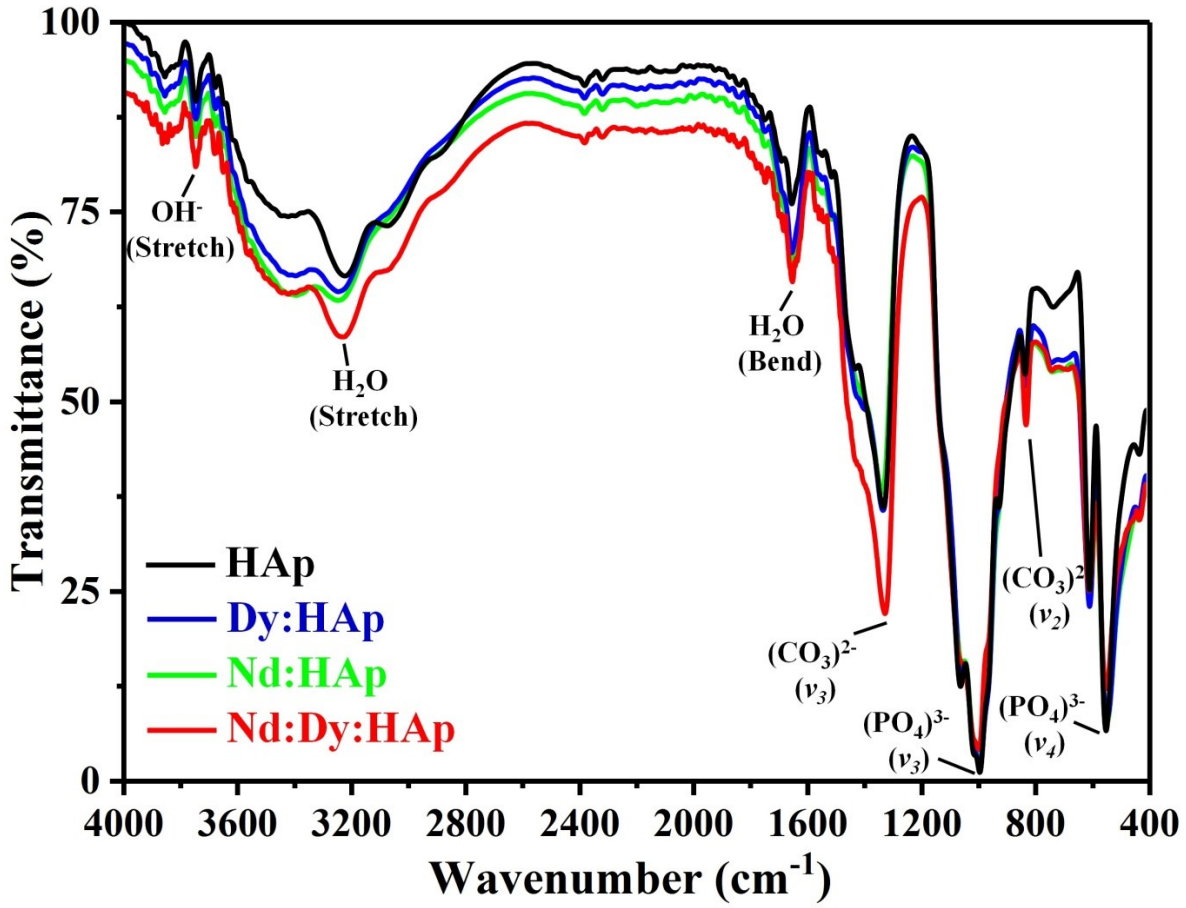

Fig. S1 FT-IR spectra of HAp, Nd:HAp, Dy:HAp, and Nd:Dy:HAp samples.

The CO_3^{2-} stretching and bending bands were located at ~1428 cm^{-1} and ~825 cm^{-1},

respectively. The v_3 vibrational mode at 1250-1530 cm^{-1} indicated the existence of minor amount of carbonate in the sample. The presence of v_3 carbonate ions (CO_3^{2-}), which were adsorbed from the atmosphere during the sample preparation, is responsible for the observed FT-IR bands. The lattice H_2O's v_2 bending mode of H-O-H is responsible for a peak at ~1645 cm^{-1}.[1,2] The stretching vibrational modes of the crystalline OH^- ions were detected as infrared bands at 3675 cm^{-1}.[1,2] Furthermore, all the samples showed characteristic stretching and bending bands of adsorbed H_2O at 2790-3720 cm^{-1} & 1590-1750 cm^{-1}. Except for the bands corresponding to adsorbed H_2O and CO_3^{2-}, whose peak intensities altered with RE metal ions doping in HAp), the FT-IR peaks of all the characteristic bands did not alter drastically with the type of RE metal ions present. However, the intensity of vibration bands of Nd:Dy:HAp are strongest among the tested samples. As the RE metals were introduced into HAp, so did the intensity of the hydroxyl group stretching bands (at 2790-3720 cm^{-1} and 3750-3800 cm^{-1}) and the carbonate group stretching bands (at 1250-1530 cm^{-1}). The FT-IR data (Table S1) of the examined HAp materials generally show that the peaks correspond to the primary vibrational modes of the HAp structure's phosphate (PO_4^{3-}), adsorbed carbonate (CO_3^{2-}), water (H–O–H), and hydroxyl (OH^-) groups. The bands' enhanced sharpness and intensity slightly when HAp was doped with RE ions, which indicates that there is a change in the crystallanity of HAp due to RE ion doping.[3] Because of the different interactions between the RE metal and other functional groups, the intensity of the characteristic bands enhanced with RE ion doping in the HAp's crystal lattice.

S2. Raman spectroscopy

Fig. S2 displays an overlay of the Raman spectra of the HAp samples that were measured in the 300 cm^{-1} – 1100 cm^{-1} range. The tetrahedral phosphate group of HAp is represented by four distinctive active vibration modes in the Raman shifts of both pure and RE doped HAp. The bending modes (v_2 & v_4) of PO_4^{3-} doubly degenerate bending create weak intensity peaks at 390 cm^{-1} – 480 cm^{-1} and 530 cm^{-1} – 690 cm^{-1}, respectively.[1,2] PO_4^{3-} has two stretching modes: a high peak at 925 cm^{-1} – 985 cm^{-1} and a faint peak at 1020 cm^{-1} – 1080 cm^{-1}. The symmetric stretching mode (v_1) and the triply degenerate asymmetric stretching mode (v_3) are involved.[1,2] The Raman signals of the HAp functional groups are displayed in Table S1, alongside the FT-IR peaks. The presence of metal dopants in the HAp structure caused slight peak shifts in the PO_4^{3-} bands. It was observed that the intensity of the vibration peak changed as the type of RE ions doped in HAp was altered.[3] The presence of characteristic phosphate functional groups in all the HAp structures was confirmed by the strong correlation between

the results of the Raman and FT-IR spectroscopy.

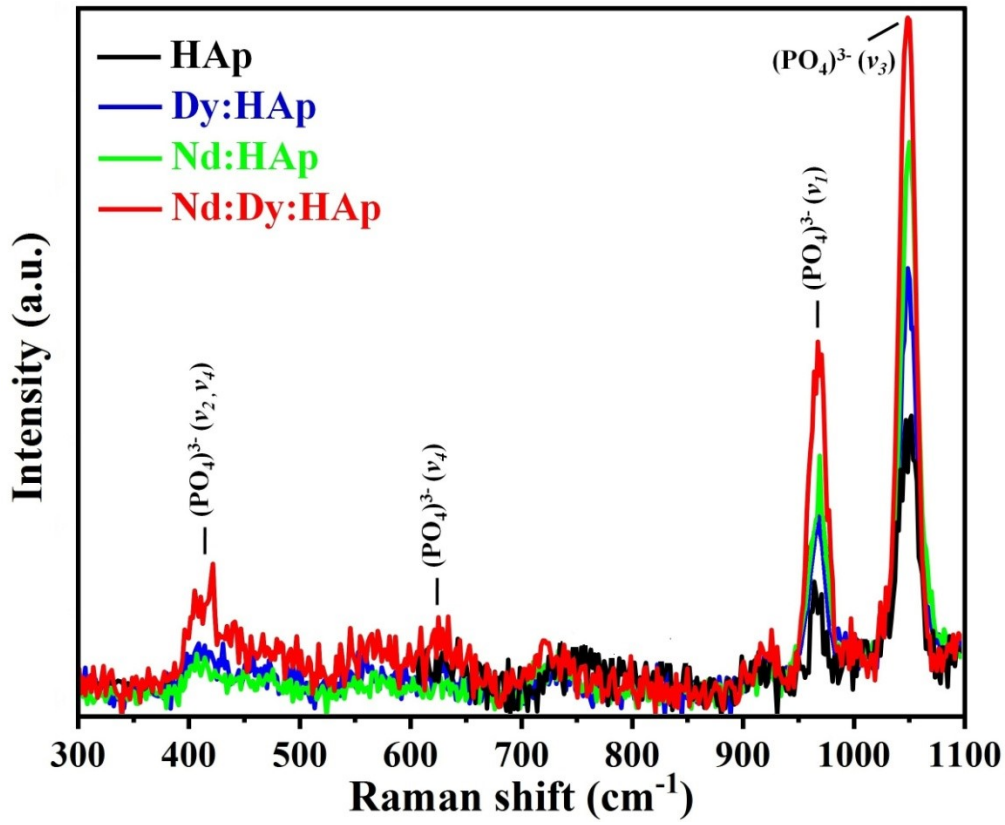

Fig. S2 Raman spectra of HAp, Nd:HAp, Dy:HAp, and Nd:Dy:HAp samples.

Table S1. A summary of FT-IR and Raman spectra peaks of HAp and Nd:Dy:HAp functional groups.

Spectroscopic	Wavenumber (cm^{-1})	Functional Groups
FT-IR	475-480	Doubly degenerate O–P–O bending (ν_2)
	570-610	Triply degenerate O–P–O bending (ν_4)
	965-970	Non-degenerate symmetric P–O stretching (ν_1)
	985-1098	Triply degenerate asymmetric P–O stretching (ν_3)
	635-740	Bending crystalline OH^-
	3750-3800	Stretching crystalline OH^-
	2790-3720 & 1590-1750	Stretching & bending of adsorbed H_2O
	1250-1530 & 810-830	Stretching C-O (ν_3) & bending (ν_2) of adsorbed CO_3^{2-}
Raman	390-480	Doubly degenerate bending, PO_4^{3-} (ν_2 & ν_4)
	530-690	Doubly degenerate bending, PO_4^{3-} (ν_4)
	925-985	Symmetric stretching, PO_4^{3-} (ν_1)
	1020-1080	Triply degenerate asymmetric stretching, PO_4^{3-} (ν_3)

S3. Atomic force microscopy

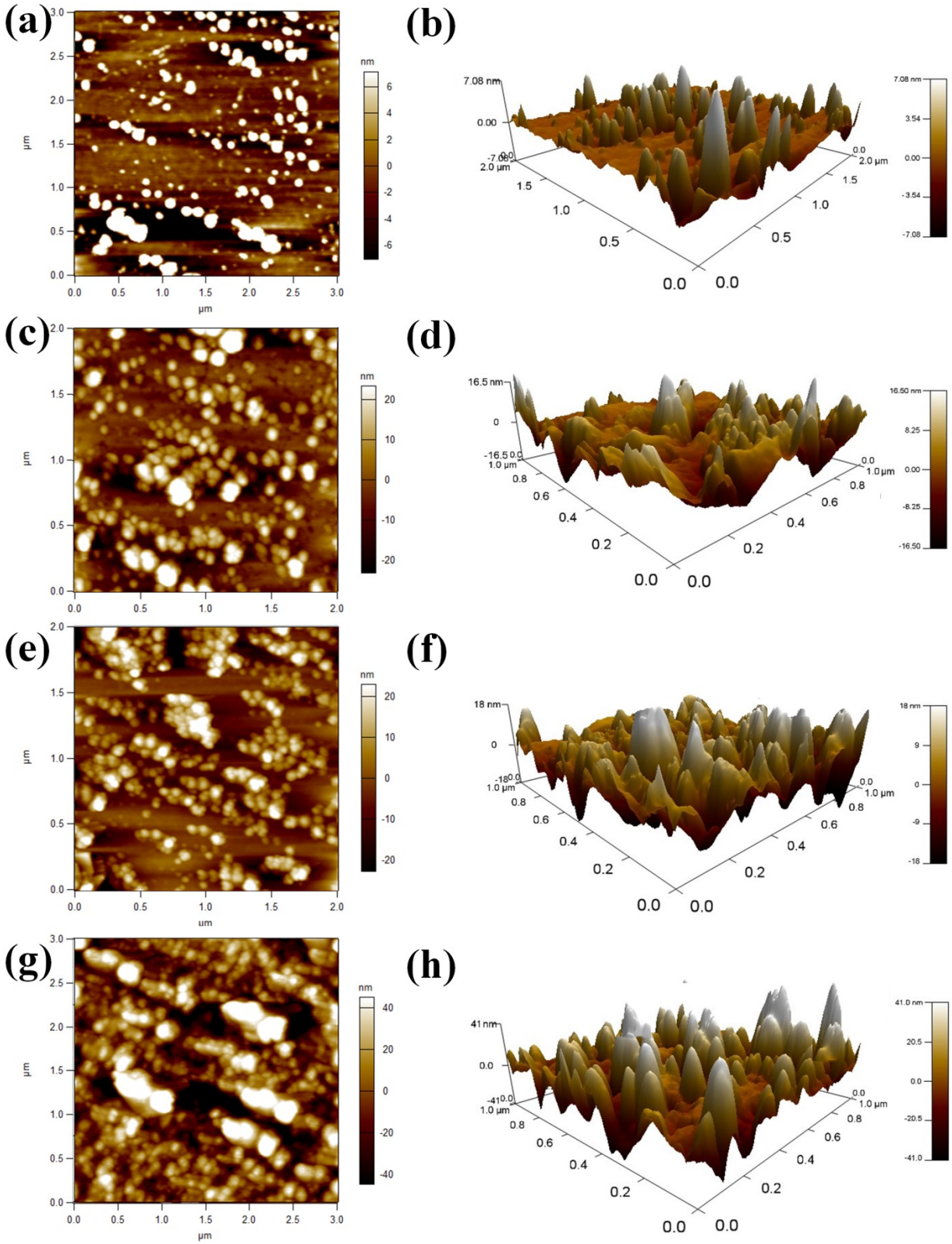

Fig. S3 AFM images (2D & 3D) of (a, b) HAp, (c, d) Nd:HAp (e, f) Dy:HAp, & (g, h) Nd:Dy:HAp.

Atomic force microscopy (AFM) has been used to examine the surface topography, surface roughness, and surface texture of the HAp, Nd:HAp, Dy:HAp, and Nd:Dy:HAp samples. 2D and 3D AFM images of all the HAp samples are presented in Fig. S3. The AFM findings

demonstrated that all the samples under investigation had uniform morphology. The 2D surface showed that there was no visible indication of fissures or cracks. From the 3D surface, it can be inferred that both HAp and RE doped HAp samples contain uniformly dispersed nanoaggregates. Gwyddion 2.60 software tool was used to calculate the surface roughness or root mean square (RRMS, R_q, or δ_{RMS}) values of the samples.[4] HAp, Nd:HAp, Dy:HAp, and Nd:Dy:HAp have δ_{RMS} values of 63.83 ± 14.19 nm, 76.60 ± 17.96, 70.61 ± 16.80, and 74.15 ± 20.99 nm, respectively. This suggests that HAp's surface is less rough than the RE doped HAp surfaces. The AFM findings are consistent with the SEM studies, which also showed smooth surfaces with no significant cracks and fissures observed in the RE-doped HAp samples.

S4. Thermal analysis

For various physical or biological applications, a material's capacity to withstand heat shock is crucial. Fig. S4 illustrates the thermal stability studies, i.e., thermogravimetry (TG) and differential thermal analysis (DTA), of HAp, Nd:HAp, Dy:HAp, and Nd:Dy:HAp were performed before the pre-thermal treatment. All the samples were heated at a rate of 5 ^oC/min, from 40 ^oC to 980 ^oC in a nitrogen (N_2) gas environment. The variations in TG weight loss is correlated with elevated temperatures to indicate the material's thermal stability.[3] The TG curves of Fig. S4(a) show significant weight reductions of 29.05 %, 27.63 %, 25.45 %, and 22.00 % for HAp, Nd:HAp, Dy:HAp, and Nd:Dy:HAp, respectively. The as-synthesized materials experience mass losses because of oxidation, dehydration, thermal breakdown, and evaporation. Small weight losses (< 5%) below 200 ^oC are caused by the evaporation of weakly entrapped water molecules from the sample surface.[5] Between 200 ^oC & 600 ^oC is when HAp and RE doped HAp undergo the majority of weight losses (20–30%). These TG transitions are associated with the removal of volatile components (solvents, crystalline H_2O, etc.) from the HAp samples.[5]

As the temperature increases to 600 °C, the TG weight loss altered proportionately with the RE doping of HAp. The TG weight loss of the samples decreased when the RE metals were doped into HAp crystal lattice structure. The thermal stability of HAp is modified by doping with Nd^{3+} and Dy^{3+} ions, which catalyzes breakdown reactions at lower temperatures. RE dopants cause the crystal lattice to be disrupted and this alters structural integrity and increases material reactivity. They have the ability to create voids and flaws, which can speed up the rate of decomposition and release volatile substances when heated. The observed

weight loss is a result of several processes working together. At temperatures above 600 °C, there are no appreciable TG weight losses observed in HAp and RE doped HAp, thus suggesting that all the HAp materials remain thermally stable even at higher temperatures. The endothermic or exothermic reactions linked to the materials' dehydration, melting, breakdown, crystallization, oxidation, and glass transition are measured by differential thermal analysis (DTA) of the as-synthesized HAp samples.

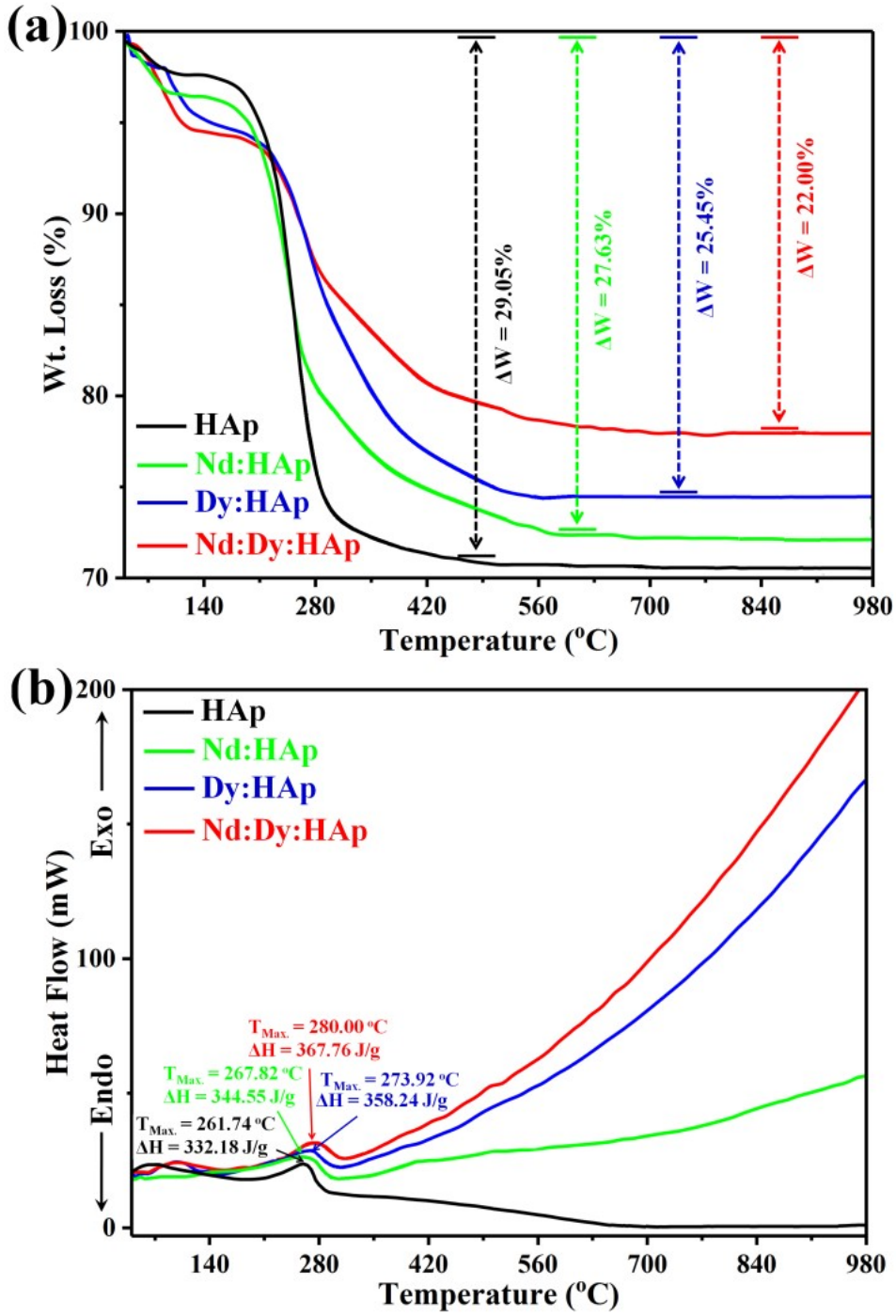

Fig. S4 Plots of (a) TG % weight loss and (b) DTA heat flow of HAp, Nd:HAp, Dy:HAp, & Nd:Dy:HAp.

From Fig. S4(b), the weight reductions shown in the TG curves are precisely represented by the DTA curves of samples.[5] Both HAp and RE doped HAp NPs exhibited a broad and medium intensity exothermic peak at ~250–350 °C. This DTA peak is because of the intra-crystalline water dehydration that results in partial oxy-HAp production.[3,6] Based on the exothermic peaks of the DTA curves, the temperature maximum ($T_{Max.}$) and change in the enthalpy (ΔH) of the transitions were determined for all the samples.[5] The exothermic peaks of HAp, Nd:HAp, Dy:HAp, and Nd:Dy:HAp have $T_{Max.}$ values of 261.74, 267.82, 273.92, and 280.00 ^{o}C and ΔH values of 332.18, 344.55, 358.24, and 367.76 J/g, respectively. The addition of RE metals to the HAp crystal lattice resulted in an increase in $T_{Max.}$ and ΔH values as well as a small shift in exothermic peaks to higher temperatures. Additionally, no further alterations to TG and DTA curves (600 to 1000 ^{o}C) suggest that the samples contain thermally stable HAp and RE doped HAp NPs.

References

1. Md. Irfan, A. Jeshurun, P. S. Suprajaa and B. M. Reddy*, J. Mater. Sci. Surf. Eng.,* 2020, **7**, 938–943. 10.jmsse/2348-8956/7-1.5.
2. Md. Irfan, P. S. Suprajaa, R. Praveen and B. M. Reddy, *Mater. Lett.,* 2021, **282**, 128685. https://doi.org/10.1016/j.matlet.2020.128685.
3. S. Mondal, V. T. Nguyen, S. Park, J. Choi, L. H. Tran, M. Yi, J. H. Shin, C. -Y. Lee, J. Oh, *Ceram. Int.,* 2020, **46**, 16020–16031. https://doi.org/10.1016/j.ceramint.2020.03.152.
4. I. Mohammad, A. Jeshurun, P. Ponnusamy and B.M. Reddy, *Mater. Today Commun.,* 2022, **331**, 04788. https://doi.org/10.1016/j.mtcomm.2022.104788.
5. J. Klinkaewnarong, E. Swatsitang and S. Maensiri, *Solid State Sci.*, 2009, **11**, 1023–1027. https://doi.org/10.1016/j.solidstatesciences.2009.02.003.
6. H. E. Khal and N. H. Batis, *New J. Chem.,* 2015, **39**, 3597–3607. https://doi.org/10.1039/C4NJ01836B.